

Clara Lauscher
Gerhard Schaldach
Markus Thommes*


Particle Generation with Liquid Carbon Dioxide Emulsions

Spray drying is a common technique for particle generation. However, due to limitations in the droplet size, the production of solid submicron particles using conventional atomizers has proven to be challenging. With the aim of overcoming this limitation, the generation and expansion of emulsions of an aqueous solution and liquid carbon dioxide with a subsequent drying step was investigated. Potassium chloride concentrations in the solution between 0.1 and 10 wt. % and mass loads of the aqueous disperse phase between 0.01 and 0.09 were used in order to study their impact on the droplet and particle size. For the lowest potassium chloride concentration, median particle diameters in the submicron size range were measured for all mass loads of the disperse phase.

Keywords: Carbon dioxide emulsion, Emulsion, Evaporation, Spray drying, Submicron particles

Received: April 11, 2022; *revised:* July 03, 2022; *accepted:* July 14, 2022

DOI: 10.1002/ceat.202200176

 This is an open access article under the terms of the Creative Commons Attribution License, which permits use, distribution and reproduction in any medium, provided the original work is properly cited.

1 Introduction

Solid particles with diameters in the submicron-size range of 0.1 to 1 μm are prevalent in many areas of life. In pharmaceutical products, the high specific surface of submicron particles can, for instance, increase the dissolution rate of poorly water-soluble drug substances [1]. Additionally, these small particles can be used by the chemical industry in paints and coatings [2].

Many techniques for producing submicron particles are known from literature. Exemplarily, the top-down approach of milling as well as the bottom-up approach of solvent removal technique have to be mentioned [3–5]. The most common of these techniques is the solvent removal technique by spray drying. In most applications, conventional atomizers such as the rotary atomizer, pressure nozzle, or two-fluid nozzle are used to disperse a liquid feed in a chamber. Solvent evaporation, forced by a hot gas stream, then leads to the formation of particles. Finally, the particles are separated from the gas stream in a cyclone and collected at its bottom [6].

Spray drying offers many advantages. For example, it is a simple, fast, and scalable technology that enables the production of powders with low moisture contents [7]. However, especially in the production of submicron particles, the spray drying technique faces challenges [6].

The separation efficiency of the cyclone is low for submicron particles due to their low mass and associated low centrifugal force [6]. The cyclone can be replaced by an electrostatic precipitator to overcome this challenge. In electrostatic precipitation, the particles in the gas stream are charged and afterwards diverted in an electrical field towards the electrode where the collection takes place [8].

A major factor is the dependency of the particle size (d_p) on the droplet size (d_d) according to Eq. (1). The particle size is also influenced by the mass fraction of the solute in the solution w_{solute} , the density ρ of the solute and the solvent, and the porosity ε [9].

$$d_p = d_d \left((1 - \varepsilon) \left(\frac{1 - w_{\text{solute}}}{w_{\text{solute}}} \frac{\rho_{\text{solute}}}{\rho_{\text{solvent}}} + 1 \right) \right)^{\frac{1}{3}} \quad (1)$$

For the generation of submicron particles, droplets in the small micrometer size range are necessary. However, with conventional atomizers, the fraction of droplets in the small micrometer size range is rather small because of limitations in workability and process conditions [10].

Other atomization processes were developed in recent years to overcome the limitations of conventional atomizers. For example, ultrasonic atomization or electrospraying can be used for the generation of droplets in the small micrometer size range, and thereby enable the production of submicron particles. Unfortunately, these techniques have the disadvantage of a low feed flow rate or a dependence on liquid electrical properties, respectively [11, 12].

Another approach for producing droplets in the small micrometer size range was introduced in a previous paper [13, 17]. As described in Fig. 1, it includes the generation of an emulsion of liquid CO_2 and a solution which is not miscible in

Clara Lauscher, Gerhard Schaldach, Prof. Dr. Markus Thommes
professors.fsv.bci@tu-dortmund.de
TU Dortmund University, Laboratory of Solids Process Engineering,
Emil-Figge-Str. 68, 44227 Dortmund, Germany.

it. Afterwards, the high-pressure emulsion is expanded through a nozzle with a small length-to-diameter ratio to force a rapid expansion of the emulsion. The liquid CO₂ evaporates as soon as the pressure drops below the saturation vapor pressure and accelerates the droplets of the solution, which presumably causes an additional droplet breakup. An aerosol consisting of gaseous CO₂ and droplets of the solution is formed, which is then dried in a downstream step to produce solid particles.

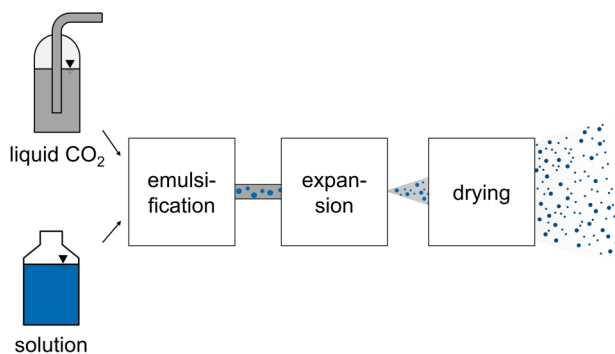


Figure 1. Schematic illustration of the investigated approach for the production of particles.

The advantage of an emulsification process in comparison to an atomization process lies in the higher density of the continuous phase. With a fixed Reynolds number, higher disintegration regimes and therefore smaller droplets can be achieved [13].

The aim of the presented study is to investigate the potential for producing small particles by nebulizing emulsions containing liquid CO₂. The experimental setup to generate and characterize the aerosols, as well as the results are presented and the latter are discussed.

2 Materials and Methods

2.1 Materials

For the preparation of the high-pressure emulsions, technical CO₂ (Messer Industriegase, Bad Soden, Germany) was used. Ultrapure water as well as solutions with concentrations of 0.1, 1, and 10 wt% of potassium chloride (KCl; Dr. Lohmann Diclean, Dortmund, Germany) in ultrapure water were investigated for the disperse phase. The surface tension, which is proportional to the work required to generate additional surface area, was determined for all solutions with a tensiometer. In accordance with literature [14], the surface tension slightly incremented with increasing concentration of KCl. Values between 72.3 and 74.9 mN m⁻¹ were measured.

2.2 Experimental Setup for Aerosol Generation and Droplet Size Measurement

The experimental setup for the droplet size measurements is displayed in Fig. 2. The liquid CO₂ was provided in a bottle

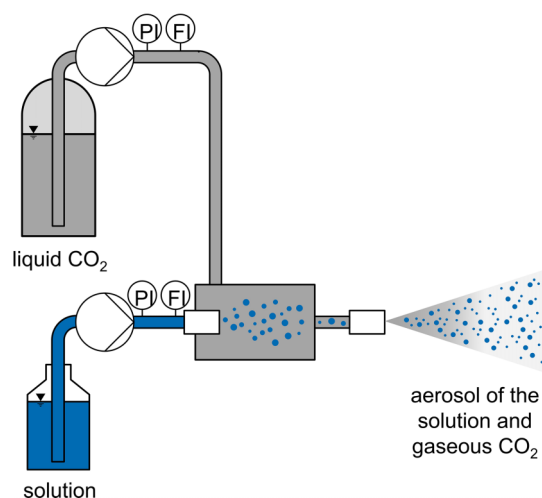


Figure 2. Experimental setup.

with a riser pipe. A gas proportioning station was used to feed the liquid CO₂ into a mixing chamber with a diameter of 20 mm and a length of 25 mm. The mass flow rate of the liquid CO₂ was set to 7.45 kg h⁻¹ and additionally monitored with a Coriolis flow meter. An HPLC pump was used to inject the water and the aqueous KCl solutions axially through the emulsification nozzle (orifice diameter: 100 μm). Flow rates of the solution between 1 and 10 mL min⁻¹ were chosen to investigate mass loads ($\mu = \dot{m}_{\text{solution}}/\dot{m}_{\text{CO}_2}$) between about 0.01 and 0.09. In combination with the KCl concentrations, mass flow rates of KCl between 0.001 and 1 g min⁻¹ were reached. The produced emulsion was nebulized through an expansion nozzle with an orifice diameter of 200 μm and a length-to-diameter ratio of 3.

In combination with the set mass flow rate of CO₂, a minimum pressure of about 80 bar was ensured allowing the CO₂ to remain in the liquid phase throughout the entire system. The droplet sizes in the resulting aerosol stream were measured 350 mm from the expansion nozzle using laser diffraction. The results shown are based on a 60-s measurement resulting in an average of 60 distributions. Thus, each replicate measurement is based on 60 discrete volumetric size distributions. The detector range was adjusted according to Mescher et al. 2010 [15] to correct for distortion of the droplet size measurement by the evaporating CO₂.

2.3 Experimental Setup for the Particle Size Measurement

A drying unit was utilized for the particle size analysis. A thin-walled pipe made of galvanized steel was placed 55 mm from the expansion nozzle. The pipe featured a diameter of 300 mm and a length of 2000 mm. Since the pipe was not capped, surrounding air was sucked into the pipe by the expanding CO₂. Two heaters with a total power consumption of about 1.2 kW were placed next to the expansion nozzle to heat the air before it was sucked in.

In addition to the laser diffractometer, an optical particle counter was used to determine particle sizes in the aerosol.

Both devices were positioned centrally at the end of the pipe. The data measured with the particle counter were based on a 60-s measurement to generate an average from ten distributions.

Further details on the previously mentioned measuring instruments and devices are summarized in Tab. 1.

Table 1. Used measuring instruments and devices.

Measuring instrument/ device	Model	Company	Origin
Tensiometer	OCA 15EC	DataPhysics Instruments	Filderstadt, Germany
Gas proportioning station	DSD/500/3.2/So	Maximator	Nordhausen, Germany
Coriolis flow meter	CORI-FLOW meter D	Bronkhorst	Kamen, Germany
HPLC pump	80 P	Knauer	Berlin, Germany
Laser diffractometer	Spraytec	Malvern Instruments	Malvern, United Kingdom
Optical particle counter	Aerosol Spectrometer and Dust Monitor 1.109	Grimm Aerosol Technik Ainring	Ainring, Germany

3 Results and Discussion

3.1 Characterization of the Drying Unit

A preliminary investigation to quantify the entrainment was conducted using multiple expansion nozzles (100, 200, and 300 μm) and different mass flow rates of CO_2 . Only combinations in which the CO_2 was in the liquid state within the expansion nozzle were selected. The total volume flow rate leaving the drying pipe was estimated using an impeller anemometer (md3/20 1178 T 100 $^\circ\text{C}$, Höntzsch, Waiblingen, Germany). The results are presented in Fig. 3. The entrained

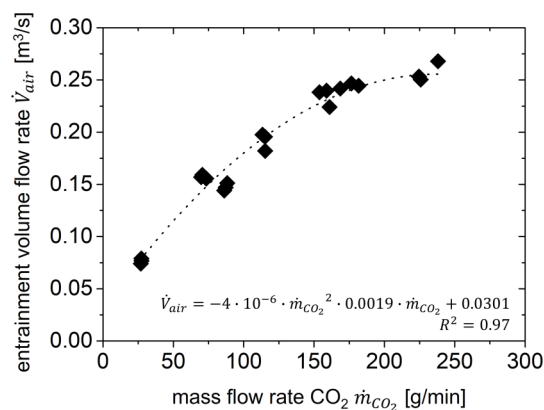


Figure 3. Entrainment of ambient air as a function of the mass flow rate of CO_2 .

volume flow rate is the total volume flow rate, under the assumption of a location-independent velocity, reduced by the volume flow rate of CO_2 under normal conditions.

With a constant specific enthalpy of evaporation, the total enthalpy of evaporation should be proportional to the mass flow rate of CO_2 . Assuming a constant temperature for all mass flow rates, the enthalpy of evaporation should cause an entrainment and acceleration of the surrounding air proportional to the mass flow rate of CO_2 . However, in Fig. 3, the slope is not constant but instead decreases with increasing mass flow rate of CO_2 . One possible explanation is the influence of the pipe. The pressure drop in turbulent flow conditions increases with higher velocity by the power of 2, reducing the energy available for acceleration. Therefore, for a constant inlet area, the entrainment volume flow rate should increase with an exponent of 2. A corresponding function was fitted and is displayed in Fig. 3.

To support the assumption of turbulent pipe flow, the velocity was measured for a single experiment at different radial positions at the outlet of the pipe. The velocities were normalized to the maximum velocity and plotted as a function of the dimensionless radial position in Fig. 4. The theoretical flow profile for turbulent flow was added for comparison, and the measured dimensionless velocities closely tracked the theoretical flow profile. Using the velocity in the center of the pipe, the Reynolds number was calculated to be about 47 000. Thus, the assumption of a turbulent pipe flow can be confirmed.

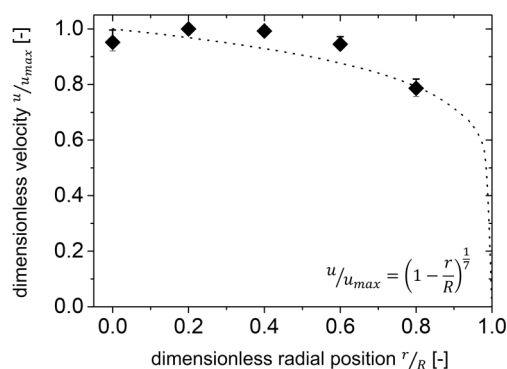


Figure 4. Dimensionless velocity at the outlet of the pipe for a water mass load of 0.08 (min, mean, max; $n = 3$) with the theoretical turbulent flow profile [16].

For further characterization of the drying unit, water was added. The drying capacity with running heaters was determined to be sufficient for the highest mass load. Laser diffraction measurements confirmed that no water droplets left the outlet of the pipe. The outlet temperature was about 28 $^\circ\text{C}$, which was 2 K lower than for the smallest water mass load of about 0.01 since the evaporation of the water consumed part of the heat power. An influence of the water mass load on the outlet velocity, and thus on the total volume flow, was also investigated. The velocity decreased with increasing water mass load from 2.8 to 2.5 m s^{-1} , because less specific energy of the CO_2 for the acceleration of the droplets is provided and a higher inertia force must be overcome.

3.2 Droplet Size Measurements

For a first characterization of the aerosol, the droplet sizes were measured for water and different KCl solutions. The median droplet diameter as a function of the mass load of the aqueous disperse phase is depicted in Fig. 5. For all disperse phases, the median droplet diameter increased with higher mass load, which was attributed to the decreasing specific energy caused by energy released by the expanding CO₂ [17]. The average median droplet diameters were between 2.9 and 7.6 μm. However, an influence of the KCl concentration on the droplet size was not observed due to only small differences in the surface tension.

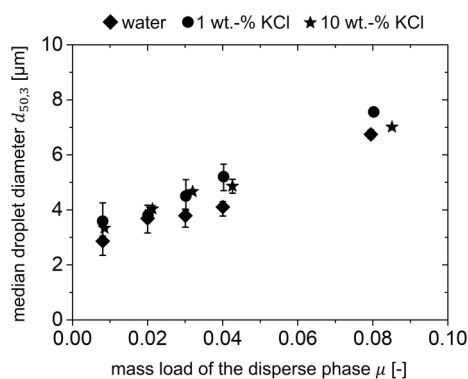


Figure 5. Median droplet diameter in the aerosol as a function of the mass load of the disperse phases water, 1 wt % KCl, and 10 wt % KCl (min, mean, max; $n \geq 2$).

3.3 Particle Size Measurements

3.3.1 Comparison of the Two Used Measurement Techniques

The use of laser diffraction for the particle size measurements was challenging due to a low particle concentration in the aerosol. Therefore, the majority of the generated aerosols had to be measured with the optical particle counter. In order to compare the droplet sizes measured with laser diffraction with the particle size measurements, a reference measurement was carried out. The highest possible light scattering could be achieved with the largest sample size. Therefore, the highest KCl concentration and the highest mass load of the aqueous disperse phase were chosen.

The results are presented in Fig. 6, and the differences between both were considered to be minor, particularly for the median particle diameter. Therefore, the particle counter was used for further particle size measurements, circumventing the inherent limitations of using laser diffraction to measure particle sizes in systems with low particle concentration.

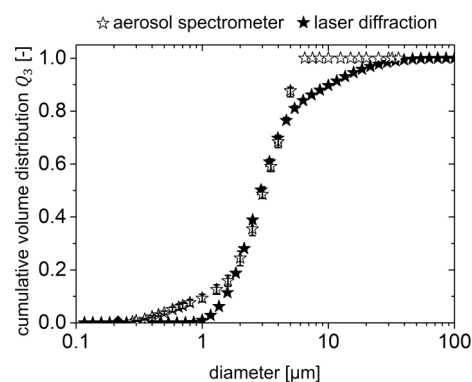


Figure 6. Cumulative mass distribution for the KCl concentration of 10 wt.% and a mass load of the disperse phase of 0.09 measured with the laser diffractometer and the optical particle counter (min, mean, max; $n = 3$).

3.3.2 Influence of the KCl Concentration on the Particle Sizes

The influence of the KCl concentration on the median particle diameter was studied for KCl concentrations of 0.1, 1, and 10 wt %. The results are illustrated in Fig. 7.

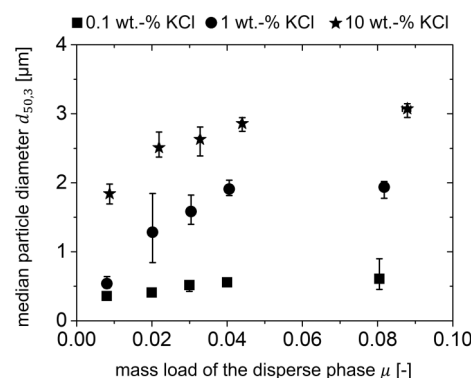


Figure 7. Median particle diameter as a function of the mass load of the disperse phase for KCl concentrations of 0.1, 1, and 10 wt % (min, mean, max; $n = 3$).

For all KCl concentrations, the particle size incremented with increasing mass load of the disperse phase as the droplet sizes previously became larger with higher mass load and the particle size is proportional to the droplet size if all other influencing variables remain constant (Fig. 5). Furthermore, the largest droplets were measured at the highest KCl concentration, which was expected according to Eq. (1). For the 0.1 wt % concentration, the average median particle diameter was between 0.4 and 0.6 μm. For the 1 wt % concentration, diameters between 0.5 and 1.9 μm were measured, and for the 10 wt % KCl concentration the average median particle diameter was found between 1.8 and 3.1 μm.

Based on Eq. (1), the porosity of the particles produced with the largest mass load and the highest KCl concentration was calculated to be 0.179, as an example. In Fig. 5, it was shown

that the droplet sizes were independent of the KCl concentration and only a function of the mass load of the disperse phase. Therefore, in accordance with Eq. (1), a concentration reduction by a factor of 10 should result in a particle size reduction by a factor of approximately 2, if all other parameters are assumed to be constant. However, the factor of about 2 was only observed for medium mass loads. The largest deviation was seen at a mass load of 0.01, which indicates a different porosity for the smallest particles.

3.3.3 Influence of the Expansion and Drying Process on Droplet and Particle Sizes

The droplet sizes in the emulsion were determined with the experimental setup and the measuring procedure described in Lauscher et al. in 2022 [17]. Since no strong influence of the KCl concentration on the droplet size in the aerosol was observed, it was assumed that small changes in the interfacial tension did not influence the droplet size in the emulsion either.

Monomodal distributions were measured for the investigated droplet and particle collectives. The largest droplets, with a median droplet diameter of about 525 μm , were measured in the emulsion. The expansion of the high-pressure emulsion and the associated evaporation of the CO_2 and acceleration of the disperse phase caused a reduction in the size of the droplets by a factor of 130. The drying process further reduced the diameter by a factor of about 2, resulting in a median droplet diameter of about 2.5 μm .

In the previous investigation [17], a correlation was found between the droplet size in the emulsion and the droplet size in the aerosol, which essentially depends on the mass load of the disperse phase (Eq. (2)).

$$d_{d,\text{aerosol}} \approx 0.0708 \mu^{0.5} d_{d,\text{emulsion}} \quad (2)$$

In combination with Eq. (1), a dependency of the particle diameter on the droplet diameter in the emulsion, the mass load of the disperse phase, and the material parameters of the KCl can be derived from this resulting in Eq. (3).

$$d_p = 0.0708 \mu^{0.5} d_{d,\text{emulsion}} \left((1 - \varepsilon) \left(\frac{1 - w_{\text{solute}}}{w_{\text{solute}}} \frac{\rho_{\text{solute}}}{\rho_{\text{solvent}}} + 1 \right) \right)^{-\frac{1}{3}} \quad (3)$$

The plausibility of this equation was subsequently proven at experimental data for a mass load of 0.02 (Fig. 8).

Inserting the median droplet diameter in the emulsion of about 525 μm into Eq. (3), a median particle diameter in the aerosol of about 2.3 μm can be calculated which is close to the measured one. The porosity $\varepsilon = 0.4$ according to Walzel [18] and the densities $\rho_{\text{KCl}} = 1980 \text{ kg m}^{-3}$ for KCl and $\rho_w = 998 \text{ kg m}^{-3}$ for water were assumed.

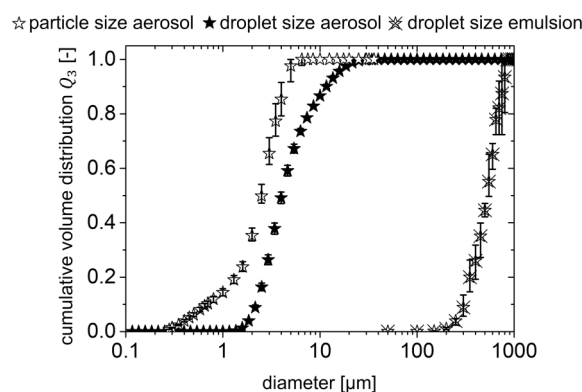


Figure 8. Cumulative volume distributions of the droplet size in the emulsion for water, the droplet size in the aerosol for 10 wt% KCl, and the dried particle size in the aerosol for the 10 wt% KCl for a mass load of 0.02 (min, mean, max; $n \geq 2$).

3.3.4 Comparison of the Particle Size with a Commercial Pneumatic Atomizer

For a further comparison with commonly used atomization processes, aerosols of the investigated solutions were produced with a commercial pneumatic atomizer (model 940, design 0, diameter 1.8 mm, Schlick, Untersiemau, Germany), since pneumatic atomizers produce the smallest droplets under conventional atomizers [10]. The solutions of 0.1, 1, and 10 wt% KCl were atomized under the same gas and liquid mass flow rates with compressed air at a pressure of 6 bar, and then dried in the drying unit described above. In Fig. 9, the resulting median droplet diameters are shown as a function of the KCl concentration in the aqueous phase. The results for the pneumatic atomizer are marked with vertical triangles. Additionally, the results for the expansion of emulsion with liquid CO_2 were added for comparison (upside down triangles).

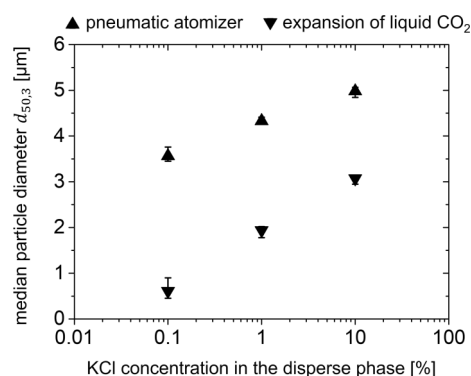


Figure 9. Median particle diameter as a function of the KCl concentration for a pneumatic atomizer and the expansion of emulsions with liquid CO_2 for a mass load between 0.08 and 0.09 (min, mean, max; $n \geq 2$).

Particles in the size range of 3.6–5 μm were produced with the pneumatic atomizer. As expected, the smallest particles were measured with the lowest concentration. By comparison,

the nebulization of emulsions with liquid CO₂ enabled the production of submicron particles for the smallest concentration. The mean droplet diameters were between 0.6 and 3.1 μm.

4 Conclusion

Nebulizing emulsions of KCl solutions and liquid CO₂ enables the continuous production of particles with a median diameter in the submicron size range. Emulsions were generated by jetting aqueous KCl solutions with concentrations between 0.1 and 10 wt% through a 100-μm orifice into the liquid CO₂, leading to mass loads between 0.01 and 0.09. Subsequently, the emulsions were expanded through an orifice with a diameter of 200 μm, resulting in an aerosol of droplets in gaseous CO₂. The solvent in the droplets was then evaporated in a drying unit. One notable feature of the drying unit is that the evaporation of the liquid CO₂ caused an entrainment of the surrounding air of about 0.2 m³ s⁻¹, and thereby increased the gas throughput in the pipe by a factor of about 170. This resulted in turbulent flow in the drying pipe.

The droplet sizes in the aerosol were measured using laser diffraction, and an effect of the KCl concentration was not observed. Only the mass load of the disperse phase influenced the droplet size in the aerosol. In total, average median droplet diameters between 2.9 and 7.6 μm were measured. The dry particles featured average median diameters between 0.4 and 3.1 μm, measured with the optical particle counter. The smallest particles resulted from the lowest KCl concentration and the smallest droplets. A comparison with a commercial pneumatic atomizer was conducted with the same mass flow rates of the gas and the aqueous phase. With a fixed mass load, it produced particles larger than the particles generated through nebulization of emulsions with liquid CO₂ by a factor of 1.6–6.

Acknowledgment

The authors thank Mr. Opie for assistance with droplet size measurements during his internship and the German Academic Exchange Service for enabling the research internship. Open access funding enabled and organized by Projekt DEAL.

The authors have declared no conflict of interest.

Symbols used

d	[m]	diameter
\dot{m}	[kg s ⁻¹]	mass flow rate
r	[m]	radial position
R	[m]	radius
u	[m s ⁻¹]	velocity
\dot{V}	[m ³ s ⁻¹]	volume flow rate
w	[-]	mass fraction

Greek letters

ε	[-]	porosity
μ	[-]	mass load
ρ	[kg m ⁻³]	density

Sub- and superscripts

d	droplet
max	maximum
min	minimum
p	particle

References

- [1] K. T. Savjani, A. K. Gajjar, J. K. Savjani, *ISRN Pharm.* **2012**, 2012, 195727. DOI: <https://doi.org/10.5402/2012/195727>
- [2] F. M. Bauers, R. Thomann, S. Mecking, *J. Am. Chem. Soc.* **2003**, 125 (29), 8838–8840. DOI: <https://doi.org/10.1021/ja034504j>
- [3] R. Al-Kassas, M. Bansal, J. Shaw, *J. Control. Release* **2017**, 260, 202–212. DOI: <https://doi.org/10.1016/j.jconrel.2017.06.003>
- [4] H.-K. Chan, P. C. L. Kwok, *Adv. Drug Deliv. Rev.* **2011**, 63 (6), 406–416. DOI: <https://doi.org/10.1016/j.addr.2011.03.011>
- [5] A. Dhiman, P. K. Prabhakar, *J. Food Eng.* **2021**, 292, 110248. DOI: <https://doi.org/10.1016/j.jfoodeng.2020.110248>
- [6] A. Sosnik, K. P. Seremeta, *Adv. Colloid Interface Sci.* **2015**, 223, 40–54. DOI: <https://doi.org/10.1016/j.cis.2015.05.003>
- [7] C. Arpagaus, A. Collenberg, D. Rütli, E. Assadpour, S. M. Jafari, *Int. J. Pharm.* **2018**, 546 (1–2), 194–214. DOI: <https://doi.org/10.1016/j.ijpharm.2018.05.037>
- [8] A. E. de Oliveira, V. G. Guerra, *Process Saf. Environ. Prot.* **2021**, 153, 422–438. DOI: <https://doi.org/10.1016/j.psep.2021.07.043>
- [9] P. Walzel, T. Furuta, in *Modern Drying Technology – Vol. 3: Product Quality and Formulation*, Wiley-VCH Verlag, Weinheim **2007**.
- [10] P. Walzel, *Design of Spraying Devices I; Short Course on Atomization and Sprays*, Darmstadt **2017**.
- [11] A. Jaworek, A. T. Sobczyk, *J. Electrostat.* **2008**, 66 (3–4), 197–219. DOI: <https://doi.org/10.1016/j.elstat.2007.10.001>
- [12] H. Liu, *Science and Engineering of Droplets*, William Andrew Publishing, Norwich, NY **1999**.
- [13] N. Czerwonatis, R. Eggers, *Chem. Eng. Technol.* **2001**, 24 (6), 619–624. DOI: [https://doi.org/10.1002/1521-4125\(200106\)24:6<619:AID-CEAT619>3.0.CO;2-H](https://doi.org/10.1002/1521-4125(200106)24:6<619:AID-CEAT619>3.0.CO;2-H)
- [14] H. Chen, Z. Li, F. Wang, Z. Wang, H. Li, *J. Chem. Eng. Data* **2017**, 62 (11), 3783–3792. DOI: <https://doi.org/10.1021/acs.jced.7b00503>
- [15] A. Mescher, P. Walzel, *Chem. Ing. Tech.* **2010**, 82 (5), 717–722. DOI: <https://doi.org/10.1002/cite.200900166>
- [16] H.-D. Voigt, in *Lagerstättentechnik* (Ed: H.-D. Voigt), Springer, Berlin **2011**.
- [17] C. Lauscher, G. Schaldach, M. Thommes, *Atomization Sprays* **2022**, 32 (4), 77–93. DOI: <https://doi.org/10.1615/AtomizSpr.2022039582>
- [18] P. Walzel, *Chem. Eng. Technol.* **2011**, 34 (7), 1039–1048. DOI: <https://doi.org/10.1002/ceat.201100051>